Comparative study on atomic ionization in bicircular laser fields by length and velocity gauges S-matrix theory *

Hong Xia(夏宏)[1], Xin-Yan Jia(贾欣燕)[1,†], Xiao-Lei Hao(郝小雷)[2], Li Guo(郭丽)[3], Dai-He Fan(樊代和)[1], Gen-Bai Chu(储根柏)[4], and Jing Chen(陈京)[5,6,‡]

[1] *School of Physical Science and Technology, Southwest Jiaotong University, Chengdu* 610031, *China*
[2] *Institute of Theoretical Physics and Department of Physics, Shanxi University, Taiyuan* 030006, *China*
[3] *State Key Laboratory for Quantum Optics and Center for Cold Atom Physics, Shanghai Institute of Optics and Fine Mechanics, Chinese Academy of Sciences, Shanghai* 201800, *China*
[4] *Science and Technology on Plasma Physics Laboratory, Laser Fusion Research Center, China Academy of Engineering Physics, Mianyang* 621900, *China*
[5] *HEDPS, Center for Applied Physics and Technology, Peking University, Beijing* 100871, *China*
[6] *Institute of Applied Physics and Computational Mathematics, Beijing* 100088, *China*

(Received 9 November 2019; revised manuscript received 9 December 2019; accepted manuscript online 12 December 2019)

Ionization of atoms in counter-rotating and co-rotating bicircular laser fields is studied using the S-matrix theory in both length and velocity gauges. We show that for both the bicircular fields, ionization rates are enhanced when the two circularly polarized lights have comparable intensities. In addition, the curves of ionization rate versus the field amplitude ratio of the two colors for counter-rotating and co-rotating fields coincide with each other in the length gauge case at the total laser intensity 5×10^{14} W/cm^2, which agrees with the experimental observation. Moreover, the degree of the coincidence between the ionization rate curves of the two bicircular fields decreases with the increasing field amplitude ratio and decreasing total laser intensity. With the help of the ADK theory, the above characteristics of the ionization rate curves can be well interpreted, which is related to the transition from the tunneling to multiphoton ionization mechanism.

Keywords: above-threshold ionization (ATI), bicircular laser fields, length gauge, velocity gauge, S-matrix theory

PACS: 32.80.Rm, 42.50.Hz **DOI:** 10.1088/1674-1056/ab610c

1. Introduction

With applications of chirped pulse amplification (CPA) technology, femtosecond or even attosecond-scale intense laser can be obtained experimentally, which allows researchers to explore the ultra-fast motion of electrons in atoms. Because the electric field generated by a strong laser beam can be compared with the Coulomb electric field felt by electrons in atoms, the interaction of the laser field with atoms or molecules can lead to many novel nonlinear phenomena, such as above-threshold ionization (ATI), nonsequential double ionization (NSDI), and high-harmonic generation (HHG). When an atom or molecule interacts with strong laser fields, an electron may absorb more photons than the minimum number of photons required for ionization and ionize. This process is called the above-threshold ionization.[1] Interestingly, this emitted electron may return to the vicinity of the parent ion under the action of laser field. When elastic scattering occurs between the emitted electron and the parent ion, the higher-order above-threshold ionization (HATI) happens.[2–4] When inelastic scattering occurs, nonsequential double ionization process appears.[5,6] Also, the electron may recombine with the parent ion and may emit a high-energy photon, which generates the high-harmonic generation.[7] This is the widely accepted "electron rescattering" three-step model proposed by Corkum and Kulander.[8,9]

It is known that the rescattering process between the photoelectron and the parent ion is favored for a linearly polarized laser field compared to circular polarization and elliptical polarization fields.[10,11] Intriguingly, the electron–ion rescattering process and the circularly polarized high-order harmonics[12,13] have been observed in the counter-rotating bicircular laser field, which makes the investigation of the strong-field nonlinear phenomena of atoms and molecules in bicircular fields attract much attention.[14] Compared with the one-dimensional trajectory of the photoelectron that returns to the parent ion in the linearly polarized field, the photoelectron trajectory for the bicircular field is in a two-dimensional (2D) plane. In addition, several control parameters are provided for this field, such as the polarization, relative intensity and phase between the two circular fields, which allows us to con-

*Project supported by the Key Laboratory Project of Computational Physics of National Defense Science and Technology of China (Grant No. 6142A05180401), the National Key Program for S&T Research and Development of China (Grant Nos. 2019YFA0307700 and 2016YFA0401100), and the National Natural Science Foundation of China (Grant Nos. 11847307, 11425414, 11504215, 11774361, and 11874246).

†Corresponding author. E-mail: xyjia@swjtu.edu.cn
‡Corresponding author. E-mail: chen_jing@iapcm.ac.cn

trol the ATI[15,16] and nonsequential double ionization process of atoms and molecules.[17,18] Moreover, bicircular fields have many applications in attosecond science, for example, bright circularly polarized soft x-ray beams can also be generated,[13] co-rotating bicircular field can be used as a spatially rotating temporal double-slit interferometer to extract the phase, amplitude information and the temporal evolution of the emitting electron wave packets.[19,20] Therefore, in this paper we focus our attention on the ionization process in a bicircular laser field, which includes the counter-rotating and co-rotating bicircular fields.

So far, many nonperturbative theoretical methods have been developed to study strong-field ionization phenomena, for example, direct numerical integration of the time-dependent Schrödinger equation (TDSE),[21–23] the semi-classical quasistatic model[8,24,25] and the quantum S-matrix theory.[26] Among them, the quantum S-matrix theory has been widely used since it has the low computational complexity and can give the clear physical picture. It is well known that the interaction between matter and electromagnetic field can be descried under two commonly accepted gauges: the velocity gauge (V gauge) and length gauge (L gauge). Because of the gauge invariance of electromagnetic action, the length and velocity gauges should give the equivalent calculation results.[27] However, due to the fact that we have to use some approximations in the S-matrix theory calculations, the results calculated under the two gauges may be gauge dependent.[28,29] For instance, photoelectron energy spectra of negative ions in linearly or circularly polarized fields calculated by the L gauge S-matrix theory are consistent with the results of TDSE[30] or experiment.[31] However, for molecules with large internuclear separation, L gauge only works well when effect of the excited state is taken into account.[32,33] Thus, in the present work we comparatively investigate the atomic ATI process in bicircular fields by the S-matrix theory in the two gauges.

In this paper, a comparative study on the above-threshold ionization of atoms in counter-rotating and co-rotating bicircular laser fields is performed, using the S-matrix theories in both length and velocity gauges. Firstly, by changing the field amplitude ratio of the two circular polarization fields with the fixing total intensity, we investigate the relationship between the atomic ionization yields and the field amplitude ratio. Secondly, by choosing four different total laser intensities of 2×10^{14} W/cm^2, 3×10^{14} W/cm^2, 4×10^{14} W/cm^2, and 5×10^{14} W/cm^2, we discuss how the relationship between the ionization yields and field amplitude ratio is affected by the total laser intensity. The paper is organized as follows. In Section 2, we define our bicircular field. In Section 3, the quantum S-matrix theory in length and velocity gauges for the atomic ATI process in bicircular fields is introduced. Results and discussions are presented in Section 4. In Section 5, our conclusion is given. It is noted that unless specified otherwise, the units used in this paper are atomic units.

2. Bicircular field

A bicircular laser field consists of two one-color circular polarized fields with different angular frequencies $r\omega$ and $s\omega$. It is defined by

$$E_X(t) = \frac{1}{\sqrt{2}}\left[E_1\sin(r\omega t+\phi_1)+E_2\sin(s\omega t+\phi_2)\right], \tag{1a}$$

$$E_Z(t) = \frac{1}{\sqrt{2}}\left[-E_1\cos(r\omega t+\phi_1)\pm E_2\cos(s\omega t+\phi_2)\right], \tag{1b}$$

where the upper sign + (the lower sign −) in Eq. (1b) corresponds to the counter-rotating (co-rotating) bicircular field. E_1 (E_2) is the amplitude of the electric field vector with frequency $r\omega$ ($s\omega$). The polarization plane of the electric field lies in the XOZ plane of the Cartesian coordinate system, laser field propagates along the Y axis. The corresponding vector potential $\boldsymbol{A}(t)$ is given by

$$\boldsymbol{E}(t) = -\partial\boldsymbol{A}(t)/\partial t, \tag{2a}$$

$$A_X(t) = \frac{1}{\sqrt{2}\omega}\left[\frac{E_1}{r}\cos(r\omega t+\phi_1)+\frac{E_2}{s}\cos(s\omega t+\phi_2)\right], \tag{2b}$$

$$A_Z(t) = \frac{1}{\sqrt{2}\omega}\left[\frac{E_1}{r}\sin(r\omega t+\phi_1)\mp\frac{E_2}{s}\sin(s\omega t+\phi_2)\right], \tag{2c}$$

in which the counter-rotating (co-rotating) bicircular field corresponds to the upper sign − (the lower sign +) in Eq. (2c). In our present work, we choose $\phi_1=\phi_2=0$, and $(r,s)=(1,2)$. Wavelengths of the fundamental and second harmonic fields are 790 nm and 395 nm, respectively. $I_1=E_1^2$ and $I_2=E_2^2$ denote the laser intensities of the fundamental and second harmonic fields. The electric field amplitude ratio of the two circular polarized fields is defined by $\rho=E_2/E_1$. Clearly the distribution of the bicircular electric field may vary with this field amplitude ratio.

In Fig. 1 we present the polar diagrams of the electric field vector $\boldsymbol{E}(t)$ for different field amplitude ratios $\rho=0.5$, 1, 6, with the total laser intensity $I=I_1+I_2=5\times10^{14}$ W/cm^2. It can be clearly seen from Fig. 1(a) that, with the increase of field amplitude ratio ρ, the absolute value of the electric field strength in the outer ring decreases and it increases gradually in the inner ring for the co-rotating field. The overall distribution of the electric field of the co-rotating field is similar to that of the circular polarized field. However, the distribution of the electric field for the counter-rotating field shows a three-lobe structure, which is more sensitive to the field amplitude ratio ρ. With the increase of the ratio ρ, although there is still a three-lobe structure distribution, it will be more and more close to the distribution of the circular polarized field. Apparently, we can see from Fig. 1 that the peak field strengths of the co-rotating and counter-rotating laser fields both reach their maxima at the field amplitude ratio $\rho=1$.

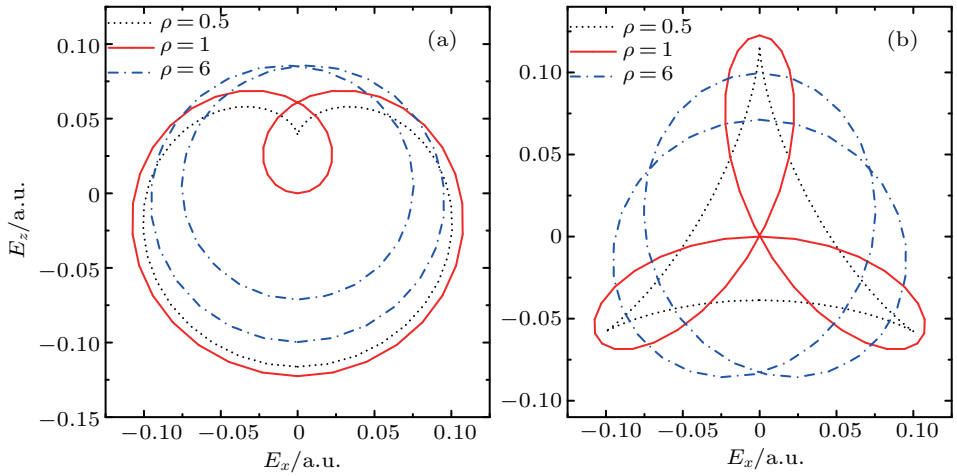

Fig. 1. Polar diagrams of the electric field vector $\boldsymbol{E}(t)$ of the bicircular laser fields for $(r,\ s) = (1,\ 2)$ and total laser intensity $I = I_1 + I_2 = 5\times10^{14}$ W/cm^2, with different field amplitude ratios $\rho = 0.5$ (black dotted curves), $\rho = 1$ (red solid curves), $\rho = 6$ (blue dot-dashed curves). Here panels (a) and (b) correspond to the co-rotating and counter-rotating bicircular fields.

3. Theory

Within the strong field approximation, the transition probability amplitude for atoms from an initial bound state $|\,\psi_{\rm i}(t)\rangle$ with ionization potential $\varepsilon_0 = E_{\rm i} = -I_{\rm P}$ to a final continuum state (Volkov state) $|\,\psi_{\rm P}(t)\rangle$ with momentum $\boldsymbol{p}$ can be written as

$$S_{\rm fi}^{\rm L} = -{\rm i}\int_{-\infty}^{\infty} {\rm d}t\,\langle\psi_{\rm P}^{\rm L}(t)|\boldsymbol{r}\cdot\boldsymbol{E}(t)|\psi_{\rm i}(t)\rangle, \tag{3a}$$

$$S_{\rm fi}^{\rm V} = -{\rm i}\int_{-\infty}^{\infty} {\rm d}t\,\langle\psi_{\rm P}^{\rm V}(t)|\hat{\boldsymbol{p}}\cdot\boldsymbol{A}(t) + \boldsymbol{A}(t)^2/2|\psi_{\rm i}(t)\rangle, \tag{3b}$$

respectively in length gauge and velocity gauge. Here $\boldsymbol{r}\cdot\boldsymbol{E}(t)$ and $\hat{\boldsymbol{p}}\cdot\boldsymbol{A}(t) + \boldsymbol{A}(t)^2/2$ are the electron–field interaction terms in the L gauge and V gauge, respectively, with $\boldsymbol{E}(t)$ the electric field vector, $\boldsymbol{A}(t)$ the vector potential, $\hat{\boldsymbol{p}} = -{\rm i}\nabla$. The initial state $\psi_{\rm i}(t) = {\rm e}^{{\rm i}I_{\rm P}t}\cdot\psi_{\rm i}(r)$ is the ground state of the atom system. In our paper, we consider a model atom which has the 1s ground state with $\psi_{\rm i}(r) = \psi_{1{\rm s}}(r) = k_1^{3/2}\cdot{\rm e}^{-k_1 r}/\sqrt{\pi}$, $k_1 = \sqrt{2I_{\rm P}}$. The Volkov wave function in the L and V gauges can be expressed as

$$\psi_{\rm P}^{\rm L}(\boldsymbol{r},t) = {\rm e}^{-{\rm i}S_{\rm P}(t)}\cdot{\rm e}^{{\rm i}(\boldsymbol{p}+\boldsymbol{A}(t))\cdot\boldsymbol{r}}/(2\pi)^{3/2}, \tag{4a}$$

$$\psi_{\rm P}^{\rm V}(r,t) = {\rm e}^{-{\rm i}S_{\rm P}(t)}\cdot{\rm e}^{{\rm i}\boldsymbol{p}\cdot\boldsymbol{r}}/(2\pi)^{3/2}, \tag{4b}$$

with the action of the electron $S_{\rm P}(t) = \frac{1}{2}\int_0^t {\rm d}\tau([\boldsymbol{p}+\boldsymbol{A}(t)]^2)$.

Substituting the vector potential of the bicircular field in Eq. (2) into the Volkov wave function in L gauge of Eq. (4a), we obtain

$$\begin{aligned}\psi_{\rm P}^{\rm L}(\boldsymbol{r},t) = (2\pi)^{-3/2}\cdot\exp\Bigg[&-{\rm i}\left(\frac{p^2}{2}+U_{\rm P1}+U_{\rm P2}\right)t\\ &-{\rm i}\left(\frac{p_X}{\sqrt{2}}\left(\frac{E_1}{(r\omega)^2}\sin(r\omega t)+\frac{E_2}{(s\omega)^2}\sin(s\omega t)\right)\right.\\ &-\frac{p_Z}{\sqrt{2}}\left(\frac{E_1}{(r\omega)^2}\cos(r\omega t)\mp\frac{E_2}{(s\omega)^2}\cos(s\omega t)\right)\\ &\left.+\frac{E_1E_2}{2rs\omega^2}\cdot\frac{1}{(r\pm s)\,\omega}\sin((r\pm s)\,\omega t)\right)\Bigg]\end{aligned}$$

$$\begin{aligned}&\times\exp\left[{\rm i}\left(\boldsymbol{p}+\boldsymbol{\epsilon}_X\left(\frac{A_1}{\sqrt{2}}\cos(r\omega t)+\frac{A_2}{\sqrt{2}}\cos(s\omega t)\right)\right.\right.\\ &\left.\left.+\boldsymbol{\epsilon}_Z\left(\frac{A_1}{\sqrt{2}}\sin(r\omega t)\mp\frac{A_2}{\sqrt{2}}\sin(s\omega t)\right)\right)\cdot\boldsymbol{r}\right],\end{aligned} \tag{5a}$$

where $U_{\rm P1} = A_1^2/4$, $U_{\rm P2} = A_2^2/4$ are the corresponding ponderomotive energies in two circular polarized fields, $A_1 = E_1/(r\omega)$, $A_2 = E_2/(s\omega)$; $p_X(p_Z)$ is the component of momentum $\boldsymbol{p}$ in the x-axis (z-axis); $\boldsymbol{\epsilon}_X$ and $\boldsymbol{\epsilon}_Z$ are unit vectors of the x-axis and z-axis, respectively. Similarly, we get the Volkov wave function in V gauge as

$$\begin{aligned}\psi_{\rm P}^{\rm V}(\boldsymbol{r},t) = \psi_{\rm P}(\boldsymbol{r})\cdot\sum\nolimits_N\sum\nolimits_{N'}\exp[-{\rm i}(p^2/2+U_{\rm P1}\\ +U_{\rm P2}-Nr\omega-N's\omega)t]\cdot J_{N,N'}(a_1,a_2,b).\end{aligned} \tag{5b}$$

Here $\psi_{\rm P}(\boldsymbol{r}) = {\rm e}^{{\rm i}\boldsymbol{p}\cdot\boldsymbol{r}}/(2\pi)^{3/2}$, and the generalized Bessel function can be expressed as

$$\begin{aligned}J_{N,N'}(a_1,a_2,b) = \sum\nolimits_{m_1}J_{m_1}(b)\,J_{N+m_1}(a_1)\,J_{N'\pm m_1}(a_2)\\ \times\exp\left[-{\rm i}\left(N\mp N'\right)x\right],\end{aligned} \tag{6}$$

with

$$\begin{aligned}x &= \arctan\left(\cos\theta/(\sin\theta\cos\varphi)\right),\\ a_1 &= \frac{A_1}{\sqrt{2}r\omega}\cdot p\sqrt{(\sin\theta\cos\varphi)^2+\cos^2\theta},\\ a_2 &= \frac{A_2}{\sqrt{2}s\omega}\cdot p\sqrt{(\sin\theta\cos\varphi)^2+\cos^2\theta},\end{aligned}$$

and $b = A_1A_2/[2(r\pm s)\,\omega]$, φ and θ are the azimuth and polar angles of the momentum $\boldsymbol{p}$ in spherical coordinates, respectively. N and N' are the photon numbers absorbed by atoms from the two circular polarized fields, respectively;[28] the $-$ $(+)$ sign in formula means the counter-rotating (co-rotating) case.

Then the transition probability amplitude in the length gauge can be obtained as follows:

$$S_{\rm fi}^{\rm L} = -{\rm i}\int_{-\infty}^{\infty}{\rm d}t\,\langle\psi_{\rm P}^{\rm L}(t)|\boldsymbol{r}\cdot\boldsymbol{E}(t)|\psi_{\rm i}(t)\rangle$$

$$
\begin{aligned}
&= -\int_{-\infty}^{\infty} \mathrm{d}t \frac{16k_1^{5/2}}{\sqrt{2}\pi} \cdot \exp\left\{ \mathrm{i} \left[\frac{p^2}{2} + U_{\mathrm{P1}} + U_{\mathrm{P2}} + I_{\mathrm{P}} \right] t \right\} \\
&\times \frac{m}{\left(k_1^2 + m^2\right)^3} \\
&\times \exp\left\{ \mathrm{i} \left[\frac{p_X}{\sqrt{2}} \left(\frac{E_1}{(r\omega)^2} \sin(r\omega t) + \frac{E_2}{(s\omega)^2} \sin(s\omega t) \right) \right.\right. \\
&- \frac{p_Z}{\sqrt{2}} \left(\frac{E_1}{(r\omega)^2} \cos(r\omega t) \mp \frac{E_2}{(s\omega)^2} \cos(s\omega t) \right) \\
&\left.\left. + \frac{E_1 E_2}{2rs\omega^2} \cdot \frac{1}{(r \pm s)\omega} \sin((r \pm s)\omega t) \right] \right\} \\
&\times \left[\left(\frac{E_1}{\sqrt{2}} \sin(r\omega t) + \frac{E_2}{\sqrt{2}} \sin(s\omega t) \right) \cdot m_{XZ} \right. \\
&\left. - \left(\frac{E_1}{\sqrt{2}} \cos(r\omega t) \mp \frac{E_2}{\sqrt{2}} \cos(s\omega t) \right) \cdot m_{ZZ} \right], \qquad (7)
\end{aligned}
$$

where

$$
\begin{aligned}
\boldsymbol{m} &= \boldsymbol{p} + \boldsymbol{\epsilon}_X \left(\frac{A_1}{\sqrt{2}} \cos(r\omega t) + \frac{A_2}{\sqrt{2}} \cos(s\omega t) \right) \\
&\quad + \boldsymbol{\epsilon}_Z \left(\frac{A_1}{\sqrt{2}} \sin(r\omega t) \mp \frac{A_2}{\sqrt{2}} \sin(s\omega t) \right), \\
m_{XZ} &= \cos\varphi_m \sin\theta_m, \\
m_{ZZ} &= \cos\theta_m, \qquad (8)
\end{aligned}
$$

φ_m and θ_m are the azimuth and polar angles of the vector $\boldsymbol{m}$ in spherical coordinates, respectively.

Also, we can obtain the transition probability amplitude in the velocity gauge

$$
\begin{aligned}
S_{\mathrm{fi}}^{\mathrm{V}} &= -\mathrm{i}2\pi \left| \langle \psi_{\mathrm{P}}(\boldsymbol{r}) | \psi_{\mathrm{i}}(\boldsymbol{r}) \rangle \right| \\
&\times \sum_{N,N'} \left(\delta\left(\frac{p^2}{2} + U_{\mathrm{P1}} + U_{\mathrm{P2}} + I_{\mathrm{P}} - Nr\omega - N's\omega \right) \right. \\
&\left. \times \left(U_{\mathrm{P1}} + U_{\mathrm{P2}} - Nr\omega - N's\omega \right) \cdot J_{N,N'}(a_1, a_2, b) \right), \qquad (9)
\end{aligned}
$$

with

$$
\begin{aligned}
\left| \langle \psi_{\mathrm{P}}(\boldsymbol{r}) | \psi_{\mathrm{i}}(\boldsymbol{r}) \rangle \right| &= \left| (2\pi)^{-3/2} \int \mathrm{e}^{-\mathrm{i}\boldsymbol{p}\cdot\boldsymbol{r}} \cdot \psi_{1\mathrm{s}}(r)\, \mathrm{d}\boldsymbol{r} \right| \\
&= 4k_1^{5/2} \cdot \pi^{-1} \cdot \left(p^2 + k_1^2 \right)^{-2}.
\end{aligned}
$$

Ponderomotive energy of the bicircular field U_{P} is the sum of the $U_{\mathrm{P}i}$ of each field,[28] i.e., $U_{\mathrm{P}} = U_{\mathrm{P1}} + U_{\mathrm{P2}}$. Ionization occurs when the electron absorbs more photon energy from the field than the sum of the ionization potential and the ponderomotive energy, i.e., $(Nr + N's)\,\omega > I_{\mathrm{P}} + U_{\mathrm{P}}$. Then the total ionization rate Γ of atoms in intense fields can be calculated in the two gauges:

$$
\Gamma = \iiint p^2 \cdot w\, \mathrm{d}p \cdot \sin\theta \mathrm{d}\theta \mathrm{d}\varphi \qquad (10)
$$

with $w = \frac{1}{t} |S_{\mathrm{fi}}|^2$.

4. Results and discussion

In this paper, we study the ATI process of the model atom ($I_{\mathrm{P}} = 0.579$ a.u., 1s ground state), by a bicircular laser field with $(r,s) = (1,2)$. The wavelengths of the fundamental and second harmonics are 790 nm and 395 nm, respectively. In our paper, each component of the bicircular fields is monochromatic, and the duration is presumed to be much longer than a laser period. In the V gauge calculations, laser field is assumed to be an infinitely long pulse. In the L gauge calculations, the pulse duration is ten optical cycles of the fundamental field. Firstly, we fix the total laser intensity as $I = 5 \times 10^{14}$ W/cm^2, and then calculate the atomic ionization rate by changing the field amplitude ratio $\rho = E_2/E_1$, the results are shown in Fig. 2. It is found that the ionization rate curves of the counter-rotating and co-rotating fields calculated by the L gauge S-matrix theory agree well with each other. When the field amplitude ratio ρ is less than one, atomic ionization rate increases as the ratio increases, it reaches its maximum at about $\rho = 1$, after that, it decreases with the increasing field amplitude ratio. That is to say, ionization rates are enhanced when the two circularly polarized lights have the comparable intensities. From the results calculated by the V gauge S-matrix theory, we also find the enhancements for both the bicircular fields when the field amplitude ratio is approximately equal to one. It is just that the ionization rate curve drops very slowly when the field amplitude ratio ρ exceeds one for the co-rotating field. However, there is a relatively large difference between the ionization rate curves of the two gauges, i.e., the rates calculated in the V gauge are 3 to 4 orders of magnitude smaller than those in the L gauge under the same conditions. This big discrepancy between the two gauges can be attributed to the gauge-invariance broken due to approximations made in the calculation process, such as neglect of ionic bounding potential and excited states. At present, this is still an open problem. The discrepancy between the two gauges varies, depending on the problems studied (see Refs. [30,34]). What gauge is superior can only be judged by comparing with the experiments or exact numerical results (i.e., TDSE). This is one of the main purposes of our manuscript. According to our calculations, the changes of the ionization rates with different conditions are qualitatively the same for both calculations given by the L and V gauges, although their magnitudes are different. In brief, the overall trends of the ionization rate curves for both the bicircular fields under the two gauges are approximately the same, whereas the magnitudes of the ionization rates calculated by the two gauges are quite different. The experiment[35] revealed that the curves of the single ionization yield versus the field amplitude ratio ρ of Ar atoms for the counter-rotating and co-rotating fields agree well with each other, which is more consistent with our L gauge results. However, for both the bicircular fields, the observed single ioniza-

tion yields have slightly decreased as the field amplitude ratio ρ increases, i.e., there are no enhancements in the experimental single ionization yield curves, which is inconsistent with our calculations by the S matrix theory in both the gauges. The probable reason may be that the enhancements of the ionization rate curves are not so prominent, especially for the length gauge-curves, where the peaks are just about 3 times higher compared with the minima in the ionization rate curves. Due to the calibration of laser intensity, this enhancement in ionization rate curve may not be detected experimentally.

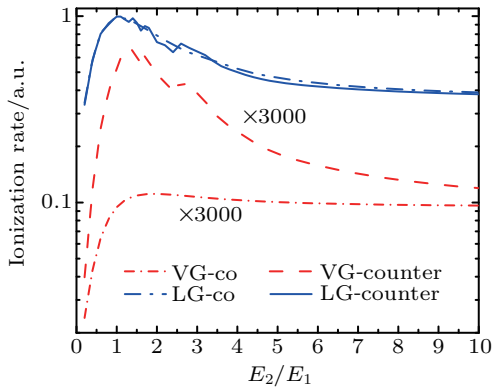

Fig. 2. Ionization rates as a function of the field amplitude ratio $\rho = E_2/E_1$, calculated by the S-matrix theory in both the L gauge and V gauge, with the fixing total laser intensity 5×10^{14} W/cm^2. Blue solid and blue dot-dashed curves correspond to the counter-rotating and co-rotating field in the L gauge case, red dashed and red short dot-dashed curves are for the counter-rotating and co-rotating field in V gauge. The ionization rates in the V gauge have been magnified to the same extent, as shown in the figure.

In order to better understand the relationship between the single ionization yield and the field amplitude ratio ρ, we discuss the ATI process using the classical ADK theory. It is known that the Keldysh parameter $\gamma = \sqrt{2I_\mathrm{P}}/U_\mathrm{P}$ has been proposed[36] to qualitatively discuss the ionization process of atoms in the laser field. If $\gamma < 1$, then tunneling ionization will be most significant. However, if $\gamma > 1$ then multiphoton ionization will be dominated. Researchers have further developed the tunneling ionization model based on Keldysh's work, and have given a simple formula for calculating the ionization probability of atomic tunneling in strong laser fields,[28,37] which is called the ADK formula. According to the ADK theory,[38] ionization rate for an atomic system with the 1s ground state driven by the intense laser fields can be expressed as

$$w_\mathrm{ADK} = \frac{4\left(2I_\mathrm{P}\right)^2}{E}\exp\left[-\frac{2}{3E}\left(2I_\mathrm{P}\right)^{3/2}\right]. \tag{11}$$

Equation (11) shows that for a given atom, the tunneling ionization rate is determined by the instantaneous electric field E.

For both the counter-rotating and co-rotating bicircular laser fields, when the field amplitude ratios are reciprocal (for instance, $\rho = a$ and $\rho = 1/a$, a is a constant), the instantaneous electric fields are equal at every moment, which can be proved in the following. The absolute value of the field strength can be denoted by

$$|\boldsymbol{E}(t)| = \sqrt{E_X^2(t) + E_Z^2(t)}. \tag{12}$$

When $\rho = a$, $E_1 = E_0$, $E_2 = aE_0$, $E_0^2 = I/\left(1+a^2\right)$, we have

$$E_X^2(t) + E_Z^2(t) = \frac{1}{2}\left(E_0^2 + a^2E_0^2\right) \mp aE_0^2\cos\left(r\omega t \mp s\omega t\right), \tag{13}$$

when $\rho = 1/a$, $E_1 = aE_0$, $E_2 = E_0$, we also have

$$E_X^2(t) + E_Z^2(t) = \frac{1}{2}\left(a^2E_0^2 + E_0^2\right) \mp aE_0^2\cos\left(r\omega t \mp s\omega t\right), \tag{14}$$

where the upper (lower) sign $-$ $(+)$ in Eqs. (13) and (14) corresponds to the counter-rotating (co-rotating) bicircular field. For example, we choose the two field amplitude ratios $\rho = 0.5$ and $\rho = 2$ to calculate the electric field distributions in the polarization plane, as shown in Fig. 3. It can be easily seen that, for both the counter-rotating and co-rotating fields, the absolute values of the instantaneous electric field are equal at every moment for $\rho = 0.5$ and $\rho = 2$.

We plot the normalized total tunneling ionization rates calculated by the ADK theory in Fig. 4. It is found that the ionization rate curves of the counter-rotating (magenta dotted curves) and co-rotating (dark grey dashed curves) fields by the ADK theory are totally coincident. They also have the similar tendency as the results of the S-matrix calculations in the two gauges, i.e., they increase first and then decrease, peaking at around $\rho = 1$. This can be easily understood from the ADK formula (11) that ADK tunneling ionization rate is only related to the instantaneous electric field strength E. As mentioned above, the maximum of electric field strength is found at $\rho = 1$, therefore the corresponding ionization rate is highest in this case. For comparison, we also plot the normalized ionization rate curves obtained by the S-matrix theory in the two gauges in Fig. 4. The curves by the Length gauge S-matrix theory are found to be roughly coincident to the ADK calculations. When the field amplitude ratio $\rho < 2.5$, ionization rate curves obtained by the two methods agree well with each other. However, when the ratio continues to increase, the L-gauge curves deviate obviously from the ADK curves. In the V-gauge case, the ionization rate curves are also qualitatively consistent with the ADK curves except that the curve of the co-rotating field drops very slowly when the ratio exceeds one. Interestingly, it can be found obviously that, both the L-gauge and V-gauge curves deviate more and more distinctly from the ADK curves as the field amplitude ratio increases. In addition, unlike the results of the ADK theory, the ionization rates of $\rho = a$ and $\rho = 1/a$ calculated by the S-matrix theory are unequal for the two bicircular fields. Next, we analyze the reasons why the above phenomena appear.

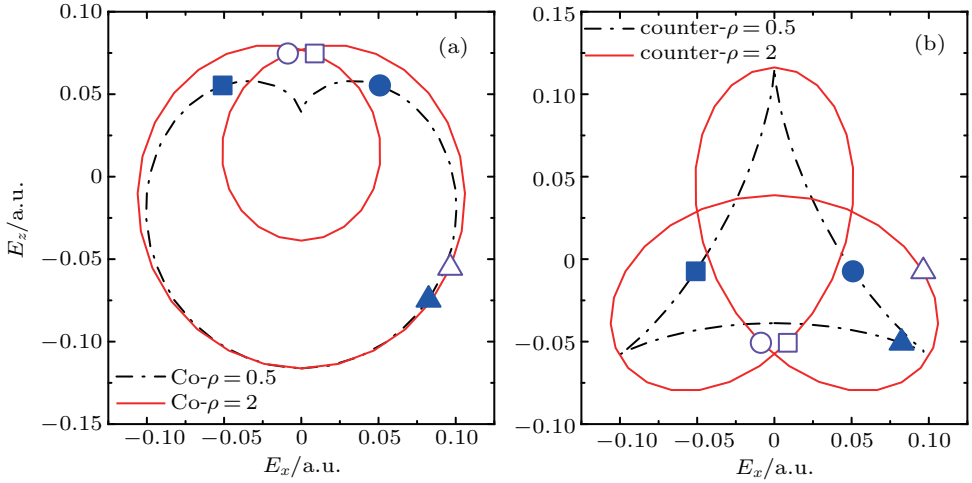

Fig. 3. Polar diagrams of the electric field vector $\boldsymbol{E}(t)$ of the bicircular laser field for $(r, s) = (1, 2)$ with total laser intensity $I = 5 \times 10^{14}$ W/cm^2, the electric field amplitude ratio $\rho = 0.5$ (black dot-dashed curves), $\rho = 2$ (red solid curves). Here panels (a) and (b) denote the field distributions of the co-rotating and counter-rotating bicircular fields. The filled (open) triangle symbol, circular symbol, square symbol represents the electric field distributions in the case of $\rho = 0.5$ ($\rho = 2$) at $t = 0.1T$, $t = 0.3T$, and $t = 0.7T$, respectively.

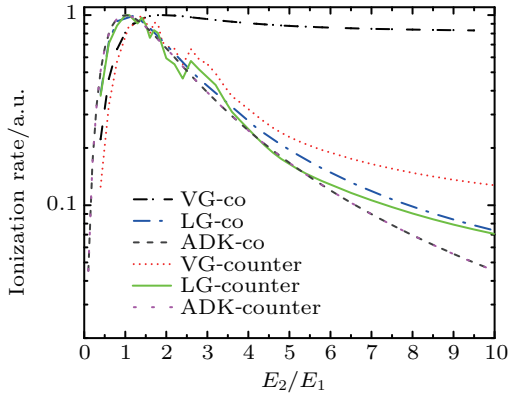

Fig. 4. Normalized ionization rates of our model atom versus field amplitude ratio E_2/E_1, with the total laser intensity 5×10^{14} W/cm^2, calculated by the ADK formula, S-matrix theory in L gauge and V gauge. The magenta dotted curve (dark grey dashed curve) describes the ionization rate of counter-rotating (co-rotating) field from the ADK theory; the green solid curve (blue dot-dashed curve) corresponds to the result of the counter-rotating (co-rotating) field from the S-matrix theory in L gauge; the red short dotted curve (black dot-dashed curve) denotes the result of the counter-rotating (co-rotating) field from S-matrix theory in V gauge. All the curves are normalized to one.

From the formula of Keldysh parameter $\gamma = \sqrt{I_P}/(2U_P)$, when the ponderomotive energy of the laser field decreases, Keldysh parameter γ increases. The ponderomotive energy of the bicircular field U_P as a function of the field amplitude ratio ρ is shown in Fig. 5. We find that U_P decreases as the field amplitude ratio increases: it decreases obviously in the region of $\rho < 2$, and decreases quite slowly when $\rho > 5$. Then the Keldysh parameter γ rises as the ratio ρ increases: γ grows fast in the region of < 2, and it rises quite slowly and tends to be one ($\gamma \approx 1$) gradually when $\rho > 5$. This indicates that as the field amplitude ratio ρ increases, the tunneling ionization mechanism is no longer applicable, the multiphoton ionization mechanism dominates, which makes the ADK theory invalid. This is the reason why the ionization rate curves by the S-matrix theory and ADK theory will deviate from each other, more and more distinctly with the increase of the field amplitude ratio ρ.

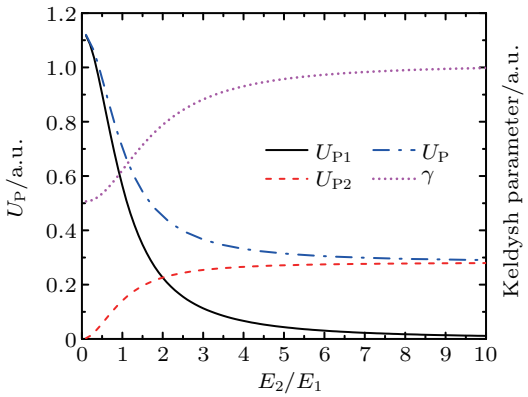

Fig. 5. Ponderomotive energy of the bicircular field U_P (blue dot-dashed curve) is shown as a function of the field amplitude ratio ρ, for the total intensity of 5×10^{14} W/cm^2. The corresponding Keldysh parameter γ is plotted by the magenta dotted curve. Black solid curve and red dashed curve denote the ponderomotive energies of the two circular field components U_{P1} and U_{P2}.

Next, we analyze the effects of the total laser intensity on the ionization rate curves calculated by the S-matrix theory in L gauge and V gauge. We choose four laser intensities 2×10^{14} W/cm^2, 3×10^{14} W/cm^2, 4×10^{14} W/cm^2, and 5×10^{14} W/cm^2 as examples. Under each laser intensity, the atomic ionization rates are calculated and analyzed by changing the field amplitude ratio ρ, the results are shown in Fig. 6. It can be seen that the L-gauge curves of the co-rotating and counter-rotating fields almost coincide at a high laser intensity of 5×10^{14} W/cm^2. The difference between the two curves of the two bicircular fields will become larger and larger when the total laser intensity decreases. When the intensity is as low as 2×10^{14} W/cm^2, the differences are quite obvious. Then, why are the two ionization rate curves of the co-rotating and counter-rotating fields more inconsistent as the total light intensity decreases? This is mainly because the lower the laser

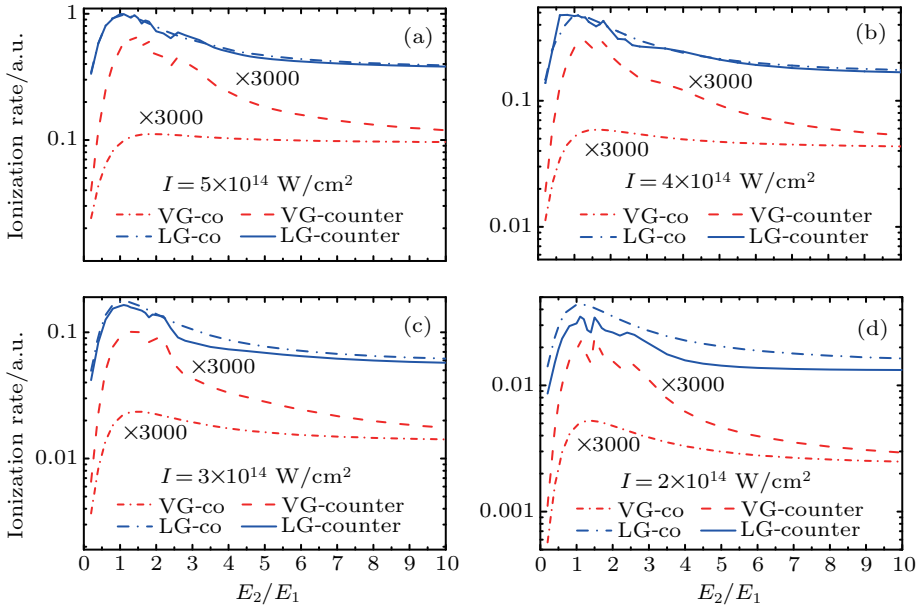

Fig. 6. Ionization rates versus the field amplitude ratios $\rho = E_2/E_1$, calculated by the S-matrix theory in both the L gauge and V gauge, with the fixing total laser intensities: (a) 5×10^{14} W/cm^2, (b) 4×10^{14} W/cm^2, (c) 3×10^{14} W/cm^2, (d) 2×10^{14} W/cm^2. In the L gauge, blue solid and blue dot-dashed curves correspond to the counter-rotating and co-rotating fields respectively. Red short-dashed and red dot-dashed curves are for the counter-rotating and co-rotating fields in V gauge. The ionization rates in V gauge have been magnified to the same extent.

field intensity, the larger the Keldysh parameter γ. This will lead to a dominance of multiphoton ionization mechanism, thus a larger deviation between the two ionization rate curves of the two bicircular fields will occur. However, it is not obvious for the V-gauge curves and there are relatively large differences between the two ionization rate curves of the two bicircular fields.

5. Conclusions

In this paper, we have made a comparative investigation of the atomic above-threshold ionization in intense counter-rotating and co-rotating bicircular laser fields, using the S-matrix theory in both the length and velocity gauges. Firstly, we study how the ionization rate of the model atom is affected by the electric field amplitude ratio ρ, when the total laser intensity is fixed at 5×10^{14} W/cm^2. It is shown that although there are obvious differences in magnitude for the ionization rate curves calculated by the two gauges S-matrix theory, they have the similar overall trend which increases first then decreases, and peaks at about $\rho = 1$. That is to say, for both bicircular fields, atomic ionization rates are enhanced when the two circularly polarized lights have almost comparable intensities. Moreover, the ionization rate curves of the counter-rotating and co-rotating fields coincide with each other better for the length gauge compared to the velocity gauge. However, the previous experiment revealed that single ionization yield curves for both the two bicircular fields agree well with each other, which are more consistent with the results calculated by the length gauge S-matrix theory. The experimentally observed single ionization yields decrease as the field amplitude ratio ρ increases for the two bicircular fields, i.e., there are no enhancements that can be found in the experimental single ionization yield curves, which are inconsistent with our theoretical calculations. The probable reason may be that the enhancements in the calculated ionization rate curves are not very notable, thus it may not be easily detected due to the calibration of laser intensity.

Then in order to better understand the results obtained by the S-matrix theory, we study the ATI process using the semiclassical ADK theory. It is shown that the ionization rate curves of the counter-rotating and co-rotating fields calculated by the ADK formula are completely coincident, and they have the same overall tendency with the S-matrix results, i.e., increasing first, peaking at $\rho = 1$ and then decreasing. This can be easily understood from the ADK theory. More interestingly, it is found that the degree of the coincidence for the two ionization curves of counter-rotating and co-rotating field decrease with the increasing field amplitude ratio or the decreasing total laser intensity. Our analysis shows that this is mainly because the Keldysh parameter γ increases when the field amplitude ratio ρ increases or the total laser intensity decreases, it will lead to a dominance of multiphoton ionization mechanism, which makes the ADK theory invalid.

References

[1] Agostini P, Fabre F, Mainfray G, Petite G and Rahman N K 1979 *Phys. Rev. Lett.* **42** 1127
[2] Paulus G G, Nicklich W, Xu H, Lambropoulos P and Walther H 1994 *Phys. Rev. Lett.* **72** 2851
[3] Lai X Y, Wang C L, Chen Y J, Hu Z L, Quan W, Chen J, Cheng Y, Xu Z Z and Becker W 2013 *Phys. Rev. Lett.* **110** 043002
[4] Zhang K, Liu M, Wang B B, Guo C Y, Yan Z C, Chen J and Liu X J 2017 *Chin. Phys. Lett.* **34** 113201

[5] Walker B, Sheehy B, DiMauro L F, Agostini P, Schafer K J and Kulander K C 1994 *Phys. Rev. Lett.* **73** 1227
[6] Larochelle S, Talebpour A and Chin S L 1998 *J. Phys. B* **31** 1201
[7] Mcpherson A, Gibson G, Jara H, Johann U, Luk T S, McIntyre I A, Boyer K and Rhodes C K 1987 *J. Opt. Soc. Am. B* **4** 595
[8] Corkum P B 1993 *Phys. Rev. Lett.* **71** 1994
[9] Schafer K J, Yang B R, DiMauro L F and Kulander K C 1993 *Phys. Rev. Lett.* **70** 1599
[10] Ben S, Wang T, Xu T, Guo J and Liu X 2016 *Opt. Express* **24** 7525
[11] Gillen G D, Walker M A and Woerkom L D V 2001 *Phys. Rev. A* **64** 043413
[12] Kfir O, Grychtol P, Turgut E, Knut R, Zusin D, Popmintchev D, Popmintchev T, Nembach H, Shaw J M, Fleischer A, Kapteyn H, Murnane M and Cohen O 2015 *Nat. Photon.* **9** 99
[13] Fan T, Grychtol P, Knut R, Hernández-García C, Hickstein D D, Zusin D, Gentry C, Dollar F J, Mancuso C A, Hogle C, Kfir O, Legut D, Carva K, Ellis J L, Dorney K, Chen C, Shpyrko O, Fullerton E E, Cohen O, Oppeneer P M, Milošević D B, Becker A, Jaroń-Becker A A, Popmintchev T, Murnane M M and Kapteyn H C 2015 *Proc. Natl. Acad. Sci. USA* **112** 14206
[14] Xia C L, Lan Y Y, Li Q Q and Miao X Y 2019 *Chin. Phys. B* **28** 103203
[15] Mancuso C A, Hickstein D D, Grychtol P, Knut R, Kfir O, Tong X M, Dollar F, Zusin D, Gopalakrishnan M, Gentry C, Turgut E, Ellis J L, Chen M C, Fleischer A, Cohen O, Kapteyn H C and Murnane M M 2015 *Phys. Rev. A* **91** 031402
[16] Huang Y, Qin C C, Zhang Y Z, Wang X C, Yan T M and Jiang Y H 2019 *Chin. Phys. B* **28** 093202
[17] Eckart S, Richter M, Kunitski M, Hartung A, Rist J, Henrichs K, Schlott N, Kang H, Bauer T, Sann H, Schmidt L P H, Schöffler M, Jahnke T and Dörner R 2016 *Phys. Rev. Lett.* **117** 133202
[18] Mancuso C A, Dorney K M, Hickstein D D, Chaloupka J L, Ellis J L, Dollar F J, Knut R, Grychtol P, Zusin D, Gentry C, Gopalakrishnan M, Kapteyn H C and Murnane M M 2016 *Phys. Rev. Lett.* **117** 133201
[19] Han M, Ge P, Shao Y, Gong Q and Liu Y 2018 *Phys. Rev. Lett.* **120** 073202
[20] Ge P, Han M, Deng Y, Gong Q and Liu Y 2019 *Phys. Rev. Lett.* **122** 013201
[21] Kulander K C 1987 *Phys. Rev. A* **35** 445(R)
[22] Hu S L, Liu M Q, Shu Z and Chen J 2019 *Phys. Rev. A* **100** 053414
[23] Xu L and Fu L B 2019 *Chin. Phys. Lett.* **36** 043202
[24] Corkum P B and Krausz F 2007 *Nat. Phys.* **3** 381
[25] Chen J, Liu J, Fu L B and Zheng W M 2000 *Phys. Rev. A* **63** 011404(R)
[26] Keldysh L V 1964 *Zh. Eksp. Teor. Fiz.* **47** 1515
[27] Faisal F H M 2007 *Phys. Rev. A* **75** 063412
[28] Reiss H R 1980 *Phys. Rev. A* **22** 1786
[29] Burlon R, Leone C, Trombetta F and Ferrante G 1987 *Nuovo Cimento D* **9** 1033
[30] Bauer D, Milošević D B and Becker W 2005 *Phys. Rev. A* **72** 023415
[31] Gazibegovic-Busuladzic A, Milošević D B and Becker W 2007 *Opt. Commun.* **275** 116
[32] Chen J and Chen S G 2007 *Phys. Rev. A* **75** 041402(R)
[33] Becker W, Chen J, Chen S G and Milošević D B 2007 *Phys. Rev. A* **76** 033403
[34] Leone C, Bivona S, Burlon R, Morales F and Ferrante G 1989 *Phys. Rev. A* **40** 1828
[35] Lin K, Jia X Y, Yu Z Q, He F, Ma J Y, Li H, Gong X C, Song Q Y, Ji Q Y, Zhang W B, Li H X, Lu P F, Zeng H P, Chen J and Wu J 2017 *Phys. Rev. Lett.* **119** 203202
[36] Delone N B and Krainov V P 1998 *Phys. Usp.* **41** 469
[37] Ammosov M V, Delone N B and Krainov V P 1986 *Sov. Phys. JETP* **64** 1191
[38] Delone N B and Krainov V P 1991 *J. Opt. Soc. Am. B* **8** 1207